(Proposal to Jefferson Lab PAC 40)

Measurement of Semi-Inclusive π° Production as Validation of Factorization

April 29, 2013

Still need to update collaboration list - placeholder

A. Camsonne, S. Covrig, P. Degtiarenko, R. Ent (spokesperson), D. Gaskell, M.K. Jones, C.E. Keppel, V. Kubarovksy, P. Nadel-Turoński, B. Sawatzky, P. Solvignon, M. Ungaro, S.A. Wood
Jefferson Lab, Newport News, VA 23606

I. Albayrak, M. Carmignotto, J. Dénes-Couto, N. Hlavin, T. Horn (co-spokesperson), F. Klein, M. Metz, B. Nepal, L. Rothgeb
The Catholic University of America, Washington, DC 20064

O. Ates, M.E. Christy, C. Jackson, N. Kalantarians, M. Kohl, P. Monaghan, A. Pushpakumari, L. Tang, J. Taylor, T. Walton
Hampton University, Hampton, VA 23668

A. Asaturyan, A. Mkrtchyan, H. Mkrtchyan (co-spokesperson), V. Tadevosyan, S. Zhamkochyan
A.I. Alikhanyan National Science Laboratory, Yerevan 0036, Armenia

C. Hyde
Old Dominion University, Norfolk, Virginia

M. Guidal, C. Munoz Camacho
Institut de Physique Nucleaire d'Orsay, IN2P3, BP 1, 91406 Orsay, France

A. Gasparian
North Carolina A&T University, Greensboro, NC 27411

M. Khandaker, V. Punjabi
Norfolk State University, Norfolk, VA 23504

F. Sabatié
CEA-Saclay, Service Physique Nucléaire, F91191 Gif-sur-Yvette, France

G.M. Huber, W. Li
University of Regina, Regina, Saskatchewan, Canada, S4S 0A2

E. Brash
Christopher Newport University, Newport News, Virginia

D. Dutta
Mississippi State University, Mississippi State, MS

G. Niculescu, I. Niculescu
James Madison University, Harrisonburg, Virginia

Y. Illieva, S. Strauch

University of South Carolina, Columbia, South Carolina

P. Markowitz. J. Reinhold
Florida International University, Miami, Florida

A. Sarty
Saint Mary's University, Halifax, Canada

P. King, J. Roche
Ohio University, Athens, OH 45701

J. Arrington, K. Hafidi, P. Reimer
Argonne National Laboratory, Argonne, IL

P. Stoler
Rensselaer Polytechnic Institute, Troy, NY 12180-3590

I. Bedlinskiy
ITEP, Moscow, Russia

and
The Neutral Particle Spectrometer collaboration
https://wiki.jlab.org/cuawiki/index.php/Collaboration

NEUTRAL PARTICLE SPECTROMETER (NPS) COLLABORATION

A. Camsonne, R. Ent, P. Nadel-Turoński, S.A. Wood, B. Wojtsekhowski
Jefferson Lab, Newport News, VA 23606

A. Asaturyan, A. Mkrtchyan, H. Mkrtchyan, V. Tadevosyan,
S. Zhamkochyan
A.I. Alikhanyan National Science Laboratory, Yerevan 0036, Armenia

M. Guidal, C. Munoz Camacho, R. Paremuzyan
Institut de Physique Nucleaire d'Orsay, IN2P3, BP 1, 91406 Orsay, France

I. Albayrak, M. Carmignotto, J. Dénes-Couto, N. Hlavin, T. Horn[1]
F. Klein, B. Nepal
The Catholic University of America, Washington, DC 20064

C. Hyde, M.N.H. Rashad
Old Dominion University, Norfolk, Virginia

P. King, J. Roche
Ohio University, Athens, OH 45701

D. Day, D. Keller, O. Rondon
University of Virginia, Charlottesville, VA, USA

D. Hamilton
University of Glasgow, Glasgow, Scotland, UK

S. Sirca
University of Ljubljana, Ljubljana, Slovenia

[1] Contact person: hornt@jlab.org

Executive Summary

The neutral pion electroproduction reaction is an important yet often neglected tool in our study of hadron structure by semi-inclusive deep inelastic scattering (SIDIS). The SU(3) wave function of π° does not allow apparent use for flavor decomposition in up and down quarks in the valence quark region, as enabled by charged-pion SIDIS processes. Yet, this same underlying wave function allows excellent use for systematic studies, to validate the prospective SIDIS science output at a 12-GeV JLab.

The exciting prospects of the SIDIS program are intertwined with our basic understanding of SIDIS at 11 GeV kinematics accessible in the high-luminosity Halls. These basic cross sections need to underpin our understanding of the anticipated factorization in hard electron-quark scattering (with dependence on Bjorken x) and the subsequent quark $\rightarrow$ pion fragmentation (with dependence on the fractional energy of the pions z), the so-called (x, z) factorization, and any subsequent dependence on low pion transverse momentum.

In SIDIS π° electroproduction, the lack of diffractive ρ contributions, the lack of pole contributions and thus radiative tail contributions at large z, the reduced nucleon resonance contribution (as for example compared to $ep \rightarrow e'\pi^-\Delta^{++}$), and the proportionality to an average fragmentation function, are all points in favor to validate low-energy (x, z) factorization required to substantiate the SIDIS science output.

To well validate the SIDIS basic framework can best be done with a magnetic spectrometer setup and correlated precisions cross sections, as well supported by the 6-GeV JLab results [1]. Here, we plan to augment a series of measurements of the transverse momentum dependence of semi-inclusive charged-pion production (E12-09-017) with neutral-pion production measurements, acquired simultaneous with a companion proposal submitted to PAC40 to measure Deep Virtual Compton Scattering (DVCS) and Deep Virtual Neutral-Pion Production (DVNP). The proposed experiment covers the same phase space in x, Q^2, z and $P_{h\perp}$ as the approved E12-09-017 experiment, and uses the same basic setup as the DVCS and DVNP companion proposal (but only a subset of kinematics and beam time).

The measurement can be well performed using the existing and well-understood Hall C High-Momentum Spectrometer to detect the scattered electrons to precisely determine the electron scattering kinematics. The neutral pion will be detected by measurement of its $\gamma\gamma$ decay products in a dedicated new neutral-pion detector. We plan to use a high-resolution lead-tungsten $PbWO_4$ detector as 25 msr neutral-pion spectrometer (NPS). The NPS will be remotely rotated using cantelevered platforms of the SHMS spectrometer. A resistive sweeping magnet of 0.3 Tm reduces electromagnetic backgrounds. A more detailed description of this setup, including realistic background simulations that show the luminosity accessible with this setup as a function of angle, is given in a separate NPS document [2]. Given that the π° acceptance and kinematics determination are predominantly determined by geometry, we anticipate high-precision ($\sim 3\%$) basic (e,e$'\pi^\circ$) cross section measurements for a 10 cm long LH2 target and a modest beam current.

The proposed cross section measurements will provide basic tests of the theoretical understanding of SIDIS in terms of factorized parton distributions and fragmentation functions. Such neutral-pion precision cross section measurements will provide a critical foundation to validate the entire SIDIS program in studying the partonic structure of the nucleon, a now-flourishing physics program at Jefferson Lab spearheaded by members of this collaboration. The collaboration is keen to augment this knowledge in the 12-GeV era, and plans to seek funding for the construction of the NPS. The total beam time request corresponds to 25 PAC days, all in parallel with a companion DVCS/DVNP proposal submitted to PAC-40 as one single run group.

Contents

I. INTRODUCTION

Much is known about the light-cone momentum fraction, x, and virtuality scale, Q^2, dependence of the up and down quark parton distribution functions (PDFs) in the nucleon. In contrast, very little is presently known beyond these one-dimensional characterizations of nucleon structure, for instance about the dependence of these functions on their transverse momentum $\mathbf{p}_T$. One of the impacts of nucleon structure beyond the one-dimensional picture is the introduction of possible orbital motion of partons.

Increasingly precise studies of the nucleon spin sum rule [3–6] strongly suggest that the net spin carried by quarks and gluons does not account completely to the net value of the spin of the nucleon, and therefore an orbital angular momentum contribution of partons to the spin of the nucleon must be significant. This in turn implies that transverse momentum of quarks should be non-zero and correlated with the spin of the nucleon itself.

Once one realizes that transverse motion of partons is important, naturally arising questions include: what are the flavor and helicity dependence of the transverse motion of quarks and gluons; what is the appropriate formalism for a description of transverse motion of quarks from a theoretical point of view; but even more important: and how can these be measured experimentally?

It has been long realized that more stringent tests of the quark-parton model arise from more exclusive hadron production experiments. In particular, processes whose common feature is the tagging of the active parton provide unique tools for probing the flavor, transverse momentum, and spatial structure of the nucleon. The most general case of those is the semi-inclusive deep inelastic scattering (SIDIS) process in which one produces any number of final-state particles and tags the one that contains the active parton.

In SIDIS there exist extra kinematical degrees of freedom associated with the detected hadron. With the positive z-axis in the direction of the electromagnetic current, two further variables can be chosen to characterize the problem: the hadron transverse momentum $P_{h\perp}$ and the elasticity z. As a result, there will be in general four structure functions for the $(e, e'\pi)$ coincidence process, the usual longitudinal and transverse structure functions and two additional interference structure functions. Measurements of the $\cos(\phi)$ and $\cos(2\phi)$ dependencies to constrain these interference structure functions are now thought to shed light on the transverse motion of quarks, assuming parton dynamics. Within this proposal, we will mostly concentrate on a $P_{h\perp}$ region where we have access to the full ϕ acceptance, such that in principle we can remove sensitivity to these interference structure functions in SIDIS kinematics by integration.

As compared to deep-inelastic scattering, the inclusive hadron production process may allow for flavor decomposition of the contributions of transverse momentum widths. This correlation has recently been more rigorously worked out as part of the transverse momentum dependent (TMD) parton distribution formalism. There are indications of an x, energy, and flavor dependence of the widths of these functions. Further understanding of the underlying parton dynamics of the SIDIS process is particularly important at the modest energies of JLab where deviations of the Leading-Order factorized picture likely contribute. The $z \to 1$ limit is here of special interest from the perspective of hadron mass corrections, both in terms of finite values of target mass M^2/Q^2 and produce hadron mass m_π^2/Q^2 relative to the virtual photon mass Q^2 (~ 4 GeV^2) [7].

Having cross section data in hand for the proposed neutral-pion SIDIS experiment, combined with the anticipated precision data for SIDIS with charged-meson production of E12-09-017, one may make comparisons between π^+, π^- and π°, which would allow for a precision verification of the often-assumed relation $\pi^\circ = (\pi^+ + \pi^-)/2$. One would anticipate that in the limit $z \to 1$ the behavior may differ from this often-used yet naive assumption given complications in the SIDIS framework at moderate energies, in the SIDIS data analysis and assumed factorization, and assumptions on the fragmentation process. In the kaon case, for example, there seems a huge difference between $D_u^{K^+}$ and $D_{\bar{s}}^{K^+}$, which naively would be the same given that $K^+ = u\bar{s}$. Of course the masses of u and s are much different, which may lead one to believe that $D_{\bar{s}} > D_u$, but the opposite seems true. In the limit $z \to 1$ one would anticipate the behavior of π° to differ from that for $(\pi^+ + \pi^-)/2$, given that the exclusive limit has no pole contributions. Thus, comparisons of π° and $\pi^\pm$ will provide valuable information on the size of non-leading twist contributions at JLab energies and potential further parton dynamics and model

extractions. As a by-product they would directly allow to revisit the inclusive-exclusive connection dating back to the 1970s in a new fashion, for instance extending the realizations within the constituent quark model of duality in several symmetry breaking scenarios from charged-pion to neutral-pion electroproduction [8]. As indicated above, semi-inclusive data in the limit of $z \to 1$ would constrain target and hadron mass corrections [7]. Lastly, the neutral-pion data would be free from various complications of the charged-pion SIDIS analysis, allowing a solid experimental validation of assumed (x, z) factorization on which any partonic interpretation of SIDIS data hinges. Thus, the proposed measurements are both of fundamental and of practical value for the SIDIS studies at JLab and beyond as they will constrain our parton interpretation of SIDIS data.

A. Factorization in semi-inclusive deep inelastic scattering.

In semi-inclusive deep inelastic scattering, a hadron h (in our case a pion) is detected in coincidence with a scattered electron, with a sufficient amount of energy and momentum transferred in the scattering process. Under the latter conditions, the reaction can be seen as knockout of a quark and subsequent (independent) hadronization.

At high values of Q^2 and ν, the cross section (at leading order in the strong coupling constant α_s) for the reaction $N(e, e'\pi)X$ can be written in the following way (see Ref. [9]),

$$\begin{aligned} \frac{\frac{d\sigma}{d\Omega_e dE_e dz dP_{h\perp}^2 d\phi}}{\frac{d\sigma}{d\Omega_e dE_e}} &= \frac{dN}{dz} b e^{-bP_{h\perp}^2} \frac{1+Acos(\phi)+Bcos(2\phi)}{2\pi}, \\ \frac{dN}{dz} &\sim \sum_i e_i^2 \; q_i(x, Q^2) \; D_{q_i \to \pi}(z, Q^2), \end{aligned} \tag{1}$$

where i denotes the quark flavor and e_i is the quark charge, and the fragmentation function $D_{q_i \to \pi}(z, Q^2)$ gives the probability for a quark to evolve into a pion π with a fraction z of the quark (or virtual photon) energy, $z = E_\pi/\nu$. The first part of this formula expresses that the cross section factorizes into the product of the virtual photon–quark interaction and the subsequent quark hadronization. A consequence of factorization is that the fragmentation function is independent of x, and the parton distribution function $q_i(x, Q^2)$ independent of z. Both parton distribution and fragmentation functions, however, depend on Q^2 through logarithmic Q^2 evolution [10]. The second part describes the dependence on the transverse momentum $P_{h\perp}$, assumed to be Gaussian, and the general dependence [11] of the cross section in the unpolarized case on the angle ϕ, the angle between the electron scattering plane and the pion production plane, with A and B, reflecting the interference terms σ_{LT} and σ_{TT}, respectively, being functions of $x, Q^2, z, P_{h\perp}$.

If one neglects the dependence of the cross section on the pion transverse momentum $P_{h\perp}$ and the angle ϕ, the SIDIS cross section as given in Eq. (1) can be written as

$$\sigma \propto \sum_i q_i(x, Q^2) \; D_{q_i \to \pi}(z, Q^2). \tag{2}$$

(At higher orders one has to worry about gluon fragmentation functions, but this can be neglected for the energy and momentum transfers under consideration here [12]). The question is how well this factorization into independent functions of x and z is fulfilled in practice.

Initial investigations of the hadronization process were made in electron–positron annihilation and in deep inelastic scattering. By now a wealth of data has been accumulated to parametrize the fragmentation functions as function of z and Q^2. It is well known that for the case of SIDIS one has to worry about separating pions directly produced by the struck quark (termed "current fragmentation") from those originating from the spectator quark system ("target fragmentation"). This has been historically done for high-energy SIDIS by using separation in rapidity, η. Early data from CERN [13, 14] suggested that a difference in rapidities, $\Delta\eta$, between pions produced in the current and target fragmentation regions ("rapidity gap") of at least $\Delta\eta \approx 2$ is needed to kinematically separate the two regions. Later, it was realized that such kinematic separation is even possible at lower energies, or low W^2, if one considers only electroproduced pions with large elasticity z, *i.e.*, with energies close to the

maximum energy transfer [14, 15]. This is what experiments at a 6-GeV or 12-GeV Jefferson Lab hinge on. In the end, factorization in terms of a hard scattering and subsequent hadronization needs to be proven experimentally, to provide a solid foundation for any partonic interpretation of SIDIS data.

At Jefferson Lab this started in Hall C, where E00-108 [16] measured the ^{1,2}H(e,e$'\pi^{\pm}$)X unseparated cross sections, predominantly at $x = 0.32$. The data conclusively showed the onset of the quark-hadron duality phenomenon in the semi-inclusive (e,e$'\pi$) process, and the relation of this to the high-energy factorization ansatz of subsequent electron-quark scattering and quark $\rightarrow$ pion production. Agreement between data and Monte Carlo simulation, based upon CTEQ5M parton distributions [17] and BKK fragmentation functions [12], was found to be excellent for $z < 0.65$ (or $M_x^2 > 2.5$ GeV^2: note that within the E00-108 kinematics $P_{h\perp} \sim 0$, and M_x^2 is almost directly related to z, as $W'^2 \equiv M_x^2 = M_p^2 + Q^2(1/x - 1)(1 - z)$. Simple ratios constructed from the data following quark-parton model descriptions were found to be remarkably close to the near-independence of z as anticipated in the high-energy limit (at leading order in α_S).

These findings have led to a rich and industrious SIDIS program at JLab at both 6 GeV, and soon 12 GeV. Nonetheless, one should keep in mind that the partonic interpretation is only as good as the experimental validation of (x, z) factorization, which we will argue is the reason to require precise neutral-pion cross section data to accompany anticipated charged-pion cross section data.

II. PHYSICS FORMALISM

The so-called Transverse Momentum Dependent (TMD) factorization was first shown [18] for Semi-Inclusive Deep Inelastic scattering (SIDIS), $lN \rightarrow l'hX$ for high values of $Q^2 \gg \Lambda_{QCD}^2$ and moderate values of transverse momenta of the produced hadron, $P_{h\perp} \sim \Lambda_{QCD}$. High Q^2 assures QCD factorization, while the small transverse momenta $P_{h\perp}$ of the electro-produced hadrons make it sensitive to intrinsic motion of the partons. The factorization is formulated in terms of so-called Transverse Momentum Dependent (TMD) parton distribution (and fragmentation functions), that in addition to their usual dependence on x and Q^2 also depend on the transverse momentum of partons $\mathbf{p}_T$.

The unpolarized SIDIS cross section [19, 20] can be written in terms of four structure functions

$$\frac{d\sigma}{dx\,dy\,d\psi\,dz\,d\phi_h\,dP_{h\perp}^2} = \frac{\alpha^2}{xyQ^2}\,\frac{y^2}{2\,(1-\varepsilon)}\left(1+\frac{\gamma^2}{2x}\right)\Big\{F_{UU,T} + \varepsilon\,F_{UU,L} + \sqrt{2\,\varepsilon(1+\varepsilon)}\,\cos\phi_h\,F_{UU}^{\cos\phi_h} + \varepsilon\cos(2\phi_h)\,F_{UU}^{2\cos\phi_h}\Big\} \tag{3}$$

where the experimentally measured structure functions are $F_{UU,T} + \varepsilon F_{UU,L}$ (separable through Rosenbluth separations as *e.g.* in experiment E12-06-104), which are ϕ_h independent, and $F_{UU}^{\cos\phi_h}$ and $F_{UU}^{2\cos\phi_h}$ which are $\cos\phi_h$ and $\cos 2\phi_h$ modulations, respectively.

At leading twist, the spin structure of a spin-1/2 hadron can be described by 8 TMDs [19–21]. Each TMD represents a particular physical aspect of spin-orbit correlations at the parton level. The dependence of the SIDIS cross section on the azimuthal angle of the electro-produced hadron with respect to the lepton scattering plane and on the nucleon polarization azimuthal angle allows a term-by-term separation of the different azimuthal contributions to the measured unpolarized and polarized cross sections and spin asymmetries. The unpolarized SIDIS cross-section can be used not only to study the unpolarized TMD distribution function $f_{q/p}(x, \mathbf{p}_T^2)$ and the unpolarized TMD fragmentation function $D_{h/q}(z, \mathbf{k}_T^2)$ that encode the intrinsic dynamics of unpolarized partons, but also the Boer-Mulders distribution and the Collins fragmentation functions, which carry information about the dynamics of transversely polarized partons inside the hadron and give rise, for instance, to a $\cos 2\phi_h$ modulation of the cross section.

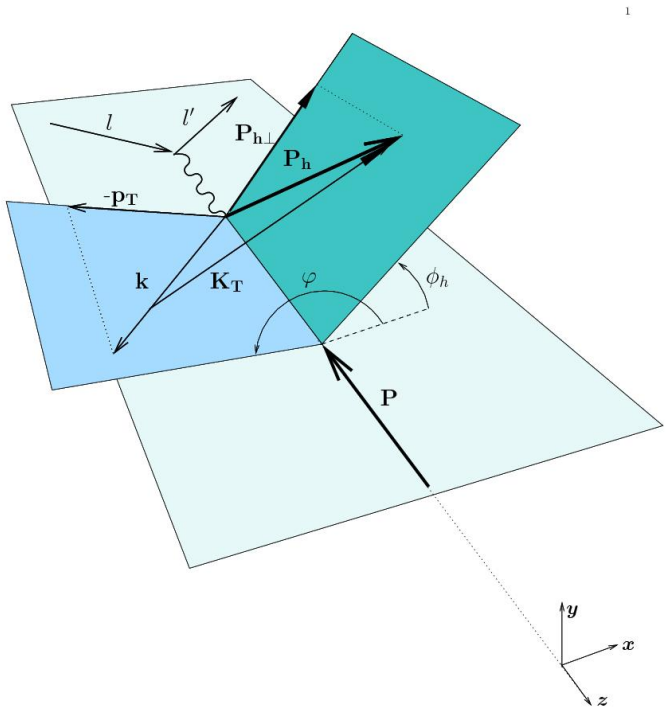

FIG. 1: Kinematics of the SIDIS process in the $\gamma^* p$ center of mass frame.

The existence of partonic intrinsic transverse momenta is unequivocally signaled by a $\cos\phi_h$ modulation, which is a subleading twist effect suppressed by one power of Q. This contribution to the unpolarized cross section consists of a purely kinematical term, the Cahn effect [22], proportional to the convolution of unpolarized distribution and fragmentation functions, together with other twist-3 contributions, as pointed out in Ref. [20].

We define here the following variables describing the kinematics:

$$\begin{aligned} s &= (p+l)^2 \quad \text{energy of the ep system} \\ W^2 &= (p+q)^2 \quad \text{energy of the } \gamma^*\text{p system} \\ Q^2 &= -q^2 > 0 \qquad \text{photon's virtuality} \end{aligned} \tag{4}$$

and

$$x = \frac{Q^2}{2\,P\cdot q}, \;\; y = \frac{P\cdot q}{P\cdot l}, \;\; z = \frac{P\cdot P_h}{P\cdot q}, \;\; \gamma = \frac{2Mx}{Q}, \;\; \varepsilon = \frac{1-y-\frac{1}{4}\gamma^2 y^2}{1-y+\frac{1}{2}y^2+\frac{1}{4}\gamma^2 y^2}. \tag{5}$$

A partonic interpretation of the measured structure functions can be obtained as convolution of distribution and fragmentation functions [19, 20]

$$F_{AB} = \mathcal{C}[w\,f\,D], \tag{6}$$

where $\mathcal{C}[...]$ is defined as

$$\mathcal{C}\big[w\,f\,D\big] = x\sum_a e_a^2 \int d^2\boldsymbol{p}_T\, d^2\boldsymbol{k}_T\, \delta^{(2)}\big(z\boldsymbol{p}_T + \boldsymbol{k}_T - \boldsymbol{P}_{h\perp}\big)\, w\left(\boldsymbol{p}_T, -\frac{\boldsymbol{k}_T}{z}\right) f^a(x,p_T^2)\, D^a(z,k_T^2), \tag{7}$$

and $w\left(\boldsymbol{p}_T, -\frac{\boldsymbol{k}_T}{z}\right)$ is a function depending on partonic momenta, $f^a(x,p_T^2)$ is a TMD parton distribution and $D^a(z,k_T^2)$ is a transverse-momentum dependent fragmentation function.

Eq. 7 indicates a summation over the various quark flavors. Thus, to go beyond and study a possible flavor dependence of the TMDs one has to measure different species of hadrons produced. This can be most readily accomplished with charged-pions and charged-kaons (and neutral pions). Within a simple gaussian Ansatz for TMDs one can show [23] that $\mathbf{P}_{h\perp} = z\mathbf{p}_T + \mathbf{k}_T$ and thus $\langle \mathbf{P}_{h\perp}^2 \rangle = z^2 \langle \mathbf{p}_T^2 \rangle + \langle \mathbf{k}_T^2 \rangle$.

The fragmentation process is traditionally described with both "favored" and "unfavored" fragmentation functions $D^+(z, \mathbf{k}_T)$ and $D^-(z, \mathbf{k}_T)$, that refer to cases when the electro-produced pion either contains or does not contain the same flavor as the struck quark. In the latter unfavored case, the quark content is picked up from the vacuum, and the process of fragmentation is suppressed.

At small values of $\mathbf{p}_T$ one expects that distribution of momenta are approximately gaussian [23] and experimental data confirm this finding. Hard QCD processes are expected to generate large non-Gaussian tails for $P_{h\perp} \gg \Lambda^2_{QCD}$. However, at small $P_{h\perp} < 0.5$ GeV, the subject of this proposal, one might use TMD factorization without worrying about gluon radiation effects. The TMDs can then be parametrized as gaussians

$$\begin{aligned} f_1^q(x, p_T^2) &= f_1^q(x) \frac{1}{\pi \langle p_T^2 \rangle} \exp\left(-\frac{\mathbf{p}_T^2}{\langle p_T^2 \rangle}\right), \\ D_{1q}^h(z, K_T^2) &= D_{1q}^h(z) \frac{1}{\pi \langle k_T^2 \rangle} \exp\left(-\frac{\mathbf{k}_T^2}{\langle k_T^2 \rangle}\right) \end{aligned} \tag{8}$$

where the widths of distributions are $\langle p_T^2 \rangle$ and $\langle k_T^2 \rangle$. Usually these widths are taken to be flavor independent, but this is just an assumption.

The two interference structure functions of Eqn. (6) introduce $\cos\phi_h$ and $\cos 2\phi_h$ modulations (with polarized beam one would introduce a fifth structure function with an associated $\sin\phi_h$ modulation that is a final-state interaction or higher-twist effect). These modulations correspond to the factors A and B in the earlier schematic Eqn. (1). TMD factorization allows for an expansion of the structure functions in powers of $1/Q$ and express them in terms of convolutions of transverse-momentum dependent distribution and fragmentation functions, alluded to above. In our case, with unpolarized structure functions, the Cahn effect and the Boer-Mulders effect come into play, with the Cahn effect (Cahn) a purely kinematical effect proportional to the quark transverse momentum, and the Boer-Mulders effect (BM) describing the correlation between the transverse polarization and transverse momentum of quarks in an unpolarized nucleon.

The longitudinal-transverse structure function $\sqrt{2\,\varepsilon(1+\varepsilon)}\cos\phi_h\, F_{UU}^{\cos\phi_h}$ is related to the $\cos\phi_h$ amplitude and suppressed as $1/Q$. Subsequent contributions are suppressed like $1/Q^3$. In the Wandzure-Wilczek approximation, the structure function has two contributions, schematically: $F_{UU}^{\cos\phi_h} \sim (1/Q)$ Cahn + $(1/Q)$ BM. Similarly, in a simplified form the transverse-transverse structure function $\varepsilon\cos(2\phi_h)\, F_{UU}^{2\cos\phi_h}$ has the following schematic dependence: $F_{UU}^{2\cos\phi_h} \sim$ BM $+(1/Q^2)$ Cahn. Recent results from both HERMES [24] and COMPASS [25] experiments find a strong z dependence of measured azimuthal asymmetries, notably at large $z > 0.5$, and a variation of positively-charged and negatively-charged pions, most noticable at large z and larger $P_{h\perp} > 0.5$ GeV, but present at smaller $P_{h\perp}$.

The possibility of a study of the k_t widths of up and down quarks under the main assumption that the fragmentation functions do not depend on quark flavor (and multiple other assumptions) was first indicated following the results of the E00-108 experiment in Hall C at Jefferson Lab [26]. Ongoing work also shows indications of an x [27] and energy [28] dependence of these k_t widths.

A recent study [28] analyzed these data in combination with the CLAS data [29], and concluded that in the kinematics similar to the CLAS data, the Hall C data could be relatively well described by a Gaussian model with average transverse momentum width of 0.24 GeV^2. The good description of the $\pi^\pm$ cross sections from different targets was argued to indicate that the assumption of flavor-independent Gaussian widths for both the transverse widths of quark and fragmentation functions was reasonable, in the valence-x region for $z = 0.55$.

This can only be considered as suggestive at best, due to the limited kinematic range covered and the assumptions. Many of these limitations could be removed with future experiments covering a wide range of Q^2 (to resolve additional higher twist contributions), full coverage in ϕ, a larger range of $P_{h\perp}$, a wide range in z (to distinguish quark width terms, weighted by powers of z, from fragmentation widths, which likely vary slowly with z), and including the π° final state for an additional consistency check (particularly on the assumption

that only two fragmentation functions are needed for charged pions from valence quarks). These goals should be attainable with the approved E12-09-017 experiment, emphasizing semi-inclusive charged-pion electroproduction. Nonetheless, analysis of semi-inclusive mesons electroproduction data at moderate energies comes with pitfalls, where a validation of the SIDIS framework is required by a companion 12-GeV program to include π° scans.

III. PITFALLS IN SIDIS ANALYSIS

Here we will describe complications in the SIDIS data analysis that warrant a precision determination of (x, z) factorization with neutral-pion data. We will first shortly revisit the empirical evidence for (x, z) factorization at 6-GeV JLab energies, and then go into some examples of the complications in the SIDIS data analysis, and why the SIDIS (e,e$'\pi^\circ$) data can further elucidate these complications and allow a quantification of the partonic interpretation of SIDIS data at a 12-GeV JLab. We will then use the extraction of the d/u ration as key example, as this has been difficult to get right in SIDIS analysis, even if the data seem to indicate to follow the SIDIS formalism.

A. Evidence for (x, z) Factorization at a 6-GeV JLab

The E00-108 experiment in Hall C was the first SIDIS experiment approved at JLab. E00-108 measured the ^{1,2}H(e,e$'\pi^\pm$)X cross sections at $x = 0.32$, and compared the measured cross sections with the results of a SIDIS simulation in Fig. 2, as a function of z [16]. The SIDIS simulation followed the high-energy factorization ansatz of subsequent electron-quark scattering, as parametrized by CTEQ5M parton distributions [17], and quark $\rightarrow$ pion production, as described in the simulation by the BKK fragmentation functions [12].

Agreement between data and Monte Carlo simulation was found to be excellent for $z < 0.65$ (or $M_x^2 > 2.5$ GeV^2: note that within the E00-108 kinematics $P_{h\perp} \sim 0$, and M_x^2 is almost directly related to z, as $W'^2 \equiv M_x^2 = M_p^2 + Q^2(1/x - 1)(1 - z)$). Hence, the large "rise" in the data with respect to the simulation at $z > 0.8$ mainly reflects the $N - \Delta(1232)$ region. Indeed, if one considers a ^{1}H(e,e$'\pi^-$)X spectrum as function of missing mass of the residual system X, one sees only one prominent resonance region, the $N - \Delta$ region. Apparently, above $M_x^2 = 2.5$ GeV^2 or so, there are already sufficient resonances to render a spectrum mimicking the smooth z-dependence as expected from the Monte Carlo simulation following the factorization ansatz. Simple ratios constructed from the data following quark-parton model descriptions were found to be remarkably close to the near-independence of z as anticipated in the high-energy limit (at leading order in α_S). Further examples of empirical evidence of the onset of a partonic interpretation of SIDIS cross sections and ratios at JLab energies, and the inherent empirical evidence for (x, z) factorization, are presented in a large archival paper [1]. It is these results that the explosion of SIDIS experiments foreseen at a 12-GeV JLab is based upon.

B. Diffractive ρ

Some of the detected events may originate from the decay of diffractive vector meson production. The underlying physics of this process, which can be described as that the virtual photon fluctuates into a vector meson, which subsequently can interact with the nucleon through multiple gluon (Pomeron) exchange, is distinctively different from the interaction of a virtual photon with a single current quark. Again, we used SIMC to evaluate such a diffractive ρ meson contribution.

The p(e,e$'\rho^\circ$)p cross section calculation was based on the PYTHIA [30] generator, adopting similar modifications as implemented by the HERMES collaboration to describe lower-energy processes [31]. Additional modifications were implemented to improve agreement with ρ^0 cross section data from CLAS in Hall B at Jefferson Lab [32].

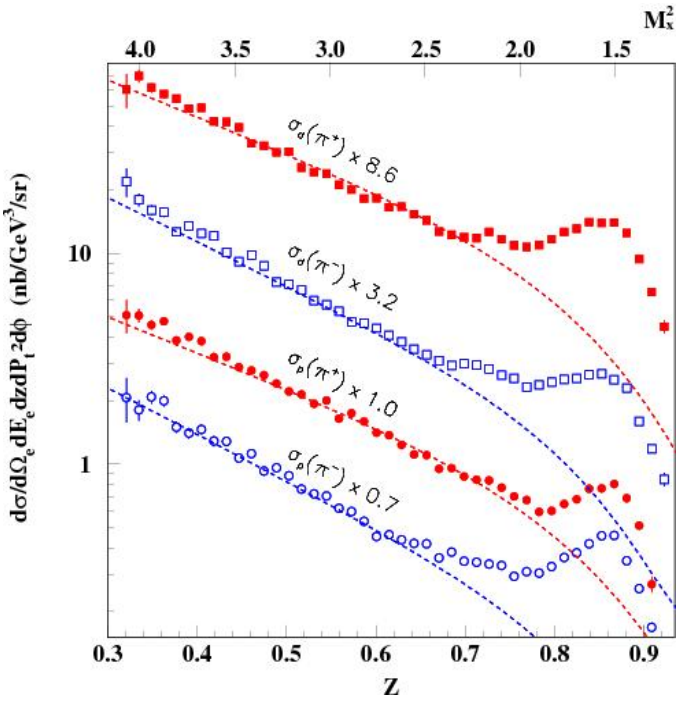

FIG. 2: The $^{1,2}H(e,e'\pi^{\pm})X$ cross sections at x=0.32 as a function of z in comparison with Monte Carlo simulations (dashed curves) starting from a fragmentation ansatz. The various cross sections have been multiplied as indicated for the purpose of plotting.

The p(e,e′ρ°)p cross section can be written as

$$\sigma^{ep\to\rho p}(\nu,Q^2) = \Gamma_T\,(1+\epsilon R)\left(\frac{M_\rho^2}{M_\rho^2+Q^2}\right)^n \sigma^{\gamma p\to\rho p}, \tag{9}$$

where Γ_T is the transverse photon flux factor, $R=\sigma_L/\sigma_T$ is the ratio of longitudinal to transverse cross sections, $\left(\frac{M_\rho^2}{M_\rho^2+Q^2}\right)^n$ ($n=2$ in PYTHIA) is an additional factor that accounts for the suppression of the cross section from virtual photons, and $\sigma^{\gamma p\to\rho p}$ is the photoproduction cross section. The modifications to the PYTHIA model implemented for this analysis mimic those implemented by the HERMES collaboration:

1. The calculation of Γ_T was performed with no high-energy approximations
2. An improved parametrization of $R=\sigma_L/\sigma_T$
3. Replacement of the exponent $n=2$ with $n\approx 2.6$, more consistent with lower energy data

The t dependence of the ρ° cross section is parametrized as

$$\frac{d\sigma}{d|t'|} = \sigma^{ep\to\rho p}(\nu,Q^2)be^{-b|t'|}, \tag{10}$$

where $t'=t-t_{min}$ (<0 for electroproduction) and b is the slope parameter. Note that at $t'=0$, b also impacts the overall scale of the forward cross section. The HERMES/PYTHIA model assumed a value of $b\approx 7$ GeV^{-2} for all energies. However, CLAS data suggested that this constant value of b did not adequately describe the t' dependence at JLab energies. The model used in SIMC fits b as a function of $c\Delta\tau$ (the vector meson formation time). Above $c\Delta\tau=2$ fm, b was taken to be a constant value of 7.0 GeV^{-2}, while for $c\Delta\tau<2$ fm, b increased from 1.0 GeV^{-2} to 7.0 GeV^{-2} between $c\Delta\tau=0.4$ fm and 2 fm.

Using the above model, the fraction of events due to pions from the decay of produced ρ mesons was estimated to range from a few percent at low z to about 15% at $z=0.6$ (see Fig. 3), and was subtracted on bin by bin basis.

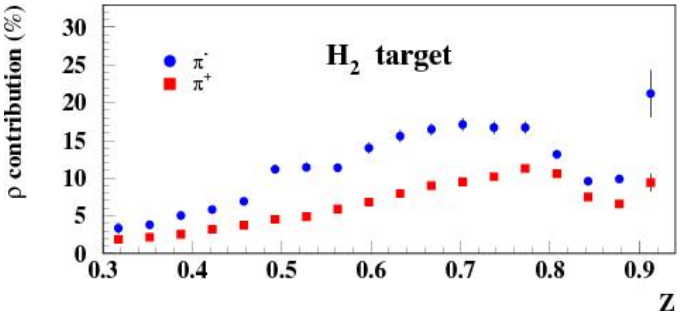

FIG. 3: Relative contribution of the events from $p(e,e'\rho^\circ)p$ reaction in Semi-Inclusive $\pi^\pm$ production experimental data for z-scan on hydrogen target.

The SIMC determination of the exclusive ρ° contribution to the semi-inclusive yield was also checked independently using a program and model developed by the CLAS collaboration [33]. The two calculations were found to agree to about the 10% level. There was uncertainty related to the choice of the parametrization for the ρ^o cross sections in the SIDIS data analysis. A slight variation (by ∼10%) of the model parameters resulted in the systematic uncertainty of up to $\approx 2.5\%$.

The advantage of SIDIS π° electroproduction is the lack of diffractive ρ contributions.

C. Radiative Tails

The radiative tail from exclusive events is the dominant correction for data at large z, $z > 0.8$ or so. For example, in the E00-108 data analysis for $z \gtrsim 0.9$ the contributions from exclusive pions become more than 50%.

Essentially all of the events that "radiate in" to a given bin come from either: (i) incoming electrons with a lower actual energy than the nominal beam energy, because they have radiated a photon; or (ii) scattered electrons with higher energy than the one measured in the spectrometer, because they radiated a photon. In both cases, the value of ν at the vertex is lower than the reconstructed one, hence z is larger and W' is smaller than the nominal value.

The radiative tails within our semi-inclusive pion electroproduction data were estimated using the Monte Carlo package SIMC. The radiative correction formula coded is based on the work of Mo and Tsai [34], which originally was derived for inclusive electron scattering, but was modified for use in coincidence experiments [35]. Details of the implementation are described in Ref. [36]. The original formulation of the radiative correction procedure used in SIMC was for $(e,e'p)$ reaction. The formula were extended to pion electroproduction by D. Gaskell [37].

As a cross-check, we also estimated radiative corrections using the code POLRAD. The standard FORTRAN code POLRAD-2.0 [38] was written for radiative correction (RC) calculations in inclusive and semi-inclusive deep-inelastic scattering of polarized leptons by polarized nucleons and nuclei. The program, which is based theoretically on the original approach proposed in the Ref. [39], was created to suit the demands of experiments with fixed polarized nuclear targets and at a collider. A new version of POLRAD [40] was created to calculate the RC for semi-inclusive (polarized) experiments. In this case the cross section depends additionally on the variable z.

The radiative corrections calculated with POLRAD-2.0 are in good agreement with SIMC. On average the RC's are on the level of $\sim 6-8\%$ for all data sets at $z < 0.7$ and reach $\sim 15\%$ at $z \gtrsim 0.9$. The relative values of radiative corrections at E00-108 kinematic settings are listed in Table I.

Exclusive Pions: Subtraction of radiative events coming from the exclusive reactions $e+p \to e'+\pi^+ +n$ and $e+n \to e'+\pi^- +p$ requires a model for the cross section of exclusive pion electroproduction that is valid for a large range of W (from the resonance region to $W \approx 2.5$ GeV) at relatively large Q^2. The model used in this analysis started with the parametrization of exclusive π^+ and π^- production cross section data from [41] at

TABLE I: The values of radiative corrections for z-scan data.

x	z	Q^2 (GeV/c)^2	π^+_H (%)	π^-_H (%)	π^+_D (%)	π^-_D (%)
0.32	0.37	2.31	1.6±0.2	3.3±0.3	2.1±0.2	3.2±0.3
0.32	0.42	2.31	2.4±0.2	4.1±0.4	2.8±0.3	3.9±0.4
0.32	0.49	2.31	3.4±0.3	5.1±0.5	3.8±0.4	4.8±0.5
0.32	0.55	2.31	4.5±0.5	6.2±0.6	4.9±0.5	5.8±0.6
0.32	0.64	2.31	5.9±0.6	7.5±0.8	6.2±0.6	7.0±0.7
0.32	0.74	2.31	7.8±0.8	9.3±0.9	8.1±0.8	8.8±0.9
0.32	0.85	2.31	10.8±1.1	11.9±1.2	11.0±1.1	11.5±1.2
0.32	0.97	2.31	18.3±1.3	18.5±1.9	18.3±1.8	18.3±1.8

TABLE II: The relative contribution of radiative exclusive tail for z-scan data.

x	z	Q^2 (GeV/c)^2	π^+_H (%)	π^-_H (%)	π^+_D (%)	π^-_D (%)
0.32	0.33	2.31	3.6±0.2	-	2.6±0.1	3.6±0.2
0.32	0.38	2.31	3.9±0.1	-	3.1±0.1	4.6±0.1
0.32	0.44	2.31	4.3±0.1	-	3.4±0.1	4.7±0.1
0.32	0.50	2.31	4.1±0.1	-	2.8±0.1	5.0±0.1
0.32	0.55	2.31	5.9±0.1	-	4.4±0.1	7.6±0.1
0.32	0.61	2.31	7.5±0.1	-	5.8±0.1	8.7±0.2
0.32	0.66	2.31	8.8±0.1	-	6.4±0.1	10.3±0.2
0.32	0.72	2.31	11.0±0.2	-	7.7±0.1	12.2±0.2
0.32	0.78	2.31	13.8±0.2	-	8.7±0.2	15.1±0.3
0.32	0.83	2.31	15.7±0.3	-	9.5±0.2	18.0±0.4
0.32	0.89	2.31	21.8±0.4	-	15.0±0.3	30.3±0.6
0.32	0.94	2.31	$\gtrsim$90	-	$\gtrsim$90	$\gtrsim$90

$W \approx 2.2$ GeV and $Q^2 = 0.7$ and 1.35 (GeV/c)^2. This parametrization describes the more recent data taken at Jefferson Lab as part of the Charged Pion Form Factor program [42–44] ($W = 1.95$ GeV, Q^2=0.6−1.6 (GeV/c)^2 and $W = 2.2$ GeV, Q^2=1.6, 2.45 (GeV/c)^2) reasonably well.

While the starting parametrization is appropriate for describing exclusive pion production above the resonance region, it does rather poorly for values of W significantly smaller than 2 GeV. Since no existing model or parametrization describes exclusive pion production both in the resonance region and at large W, we chose to adjust our starting model by-hand to give good agreement with the MAID model [45] of pion electroproduction in the resonance region. This by-hand adjustment began with the assumption that the longitudinal contribution was well described by the starting model, even at relatively low W. Discrepancies between the starting fit and the MAID calculation were attributed to the transverse cross section and were removed by assuming a more modest W dependence therein. We further simplified the model by assuming that the TT and LT interference terms mostly averaged to zero over our experimental acceptance so that they contributed negligibly to the radiative events.

We used the SIMC package with this modified model for exclusive π^+ electroproduction on the proton and for π^+ and π^- production on the deuteron for all the kinematic settings of E00-108. The contributions from exclusive pions were subtracted on a bin by bin basis. On average, the contribution from the exclusive tail was estimated to range from 5 to 15% as a function of z (at $z < 0.8$) (see Table II).

The radiative tail from exclusive events is clearly the dominant correction for the E00-108 data at $z > 0.8$. This will in general be the case for SIDIS data from JLab at 6-GeV or 12-GeV beam energies, albeit with variations with z and Q^2. For $z \gtrsim 0.9$ the contributions from exclusive pions can become more than 50%. Note that we also performed an alternative analysis using the code HAPRAD [46]. The two results agree to within $\pm 10 - 15\%$ in the relative contribution of the radiative tail due to the exclusive channels. Given the agreement

and the relative contribution, the resulting uncertainty is estimated to be at the 1% level or less (for $z < 0.8$).

The advantage of SIDIS π° electroproduction is the lack of pole contributions, and thus radiative tail contributions at large z.

D. Nucleon Resonance Contributions

As noted earlier, for E00-108 kinematics, $P_{h\perp} \sim 0$, M_x^2 is almost directly related to z Hence, as illustrated in Fig. 2, the large "rise" in the data with respect to the partonic expectations, based upon a factorization ansatz of electron-quark scattering and subsequent quark-pion fragmentation, is mainly due to the introduction of the nucleon resonance region, or more specifically the $N - \Delta(1232)$ region, at $z > 0.7$. It is important to remember that the counter of this argument is that above $M_x^2 = 2.5$ GeV^2 or so (corresponding to $z < 0.7$ within the E00-108 kinematics), there are already sufficient resonances to render a spectrum with smooth z-dependence.

At 12-GeV energies, the accessible Q^2 for fixed x slightly grows, so the z value corresponding to $M_x^2 = 2.5$ GeV^2 changes. For a doubling of Q^2, the z value for instance would grow to $z = 0.85$ (for $x = 0.32$). Similarly, the z value where a partonic interpretation of SIDIS data at JLab energies will be relevant, will depend on the meson species measured. Separation of current and target region fragmentation, assumed to be required for (x, z) factorization, will be different for pions and kaons. This will impact the lower z value where a partonic interpretation of data within a SIDIS framework is relevant for JLab energies. Similarly, at the higher z values there are differences expected due to the specific ^{1}H(e,e$'m$)X nucleon resonance spectrum. In fact, the missing mass spectrum of residual state X will be different for various mesons m. It is well known that nucleon resonance excitations are most visible for the lower-lying (ground and) first-excited states, and less visible for heavier mass mesons m. It will also be different for neutral-pions versus charged-pions, due to specific strength on nucleon resonance excitations. For example, the $ep \rightarrow e'\pi^\circ\Delta^+$ is much reduced as compared to $ep \rightarrow e'\pi^-\Delta^{++}$, giving reason to expect the SIDIS (e,e$'\pi^\circ$) cross section to be smoother at large z than the charged-pion equivalent, giving easier access to partonic interpretation.

The advantage of SIDIS π° electroproduction is the reduced nucleon resonance contribution allowing access to larger z values in partonic interpretation.

E. Fragmentation Functions

Due to the lack of a priori calculations within QCD of the fragmentation process, embodying the long-range dynamics of confinement, one typically resorts to a parameterization in terms of fragmentation functions [47]. Fragmentation functions are similar as parton distribution functions universal, *i.e.*, process independent, with their dependence on the scale Q^2 well-known in terms of QCD evolution. In general, the fragmentation functions are, for the in the valence quark region most copious up and down quarks, assumed to not depend on quark flavor. Beyond the possibility to be flavor dependent, an additional complication is that one can have favored and unfavored fragmentation functions, D^+ and D^-, respectively, that refer to the case where the electro-produced meson contains the same flavor as the struck quark or not.

With the assumptions of factorization, isospin symmetry and charge conjugation (and neglecting heavy quarks in the valence-quark region), the cross sections of $\pi^\pm$ production on protons and neutrons at fixed Q^2 can be presented as:

$$\begin{aligned}
{\sigma_p}^{\pi^+}(x,z) &\propto 4u(x)D^+(z) + d(x)D^-(z) + 4\bar{u}(x)D^-(z) + \bar{d}(x)D^+(z) \\
{\sigma_p}^{\pi^-}(x,z) &\propto 4u(x)D^-(z) + d(x)D^+(z) + 4\bar{u}(x)D^+(z) + \bar{d}(x)D^-(z) \\
{\sigma_n}^{\pi^+}(x,z) &\propto 4d(x)D^+(z) + u(x)D^-(z) + 4\bar{d}(x)D^-(z) + \bar{u}(x)D^+(z) \\
{\sigma_n}^{\pi^-}(x,z) &\propto 4d(x)D^-(z) + u(x)D^+(z) + 4\bar{d}(x)D^+(z) + \bar{u}(x)D^-(z),
\end{aligned} \tag{11}$$

with D^+ and D^- the favored and unfavored fragmentation functions defined as $D^+ = D_u^{\pi^+} = D_{\bar{d}}^{\pi^-}$, and $D^- = D_u^{\pi^-} = D_{\bar{d}}^{\pi^+}$, respectively.

In general, the SIDIS charged-pion electroproduction cross sections, including their ratios, will both depend on the favored and unfavored fragmentation functions, or their respective ratios. In contrast, the neutral pion plays a different role due to its specific quark substructure, and the SIDIS neutral-pion electroproduction cross section will be related to the average of the two (D^+ and D^-) fragmentation functions. A similar result, under the assumption of flavor indepedence of the fragmentation functions, would follow from the often-used relation $\sigma^{\pi^\circ}(x,z) = [\sigma^{\pi^+}(x,z) + \sigma^{\pi^-}(x,z)]/2$.

The advantage of SIDIS π° electroproduction is the proportionality to an average fragmentation function.

F. The Problem Child: d/u Ratio

The measured cross sections or yields for $\pi^\pm$ production on the proton and deuteron can in the quark-parton model be directly used to form relations in terms of the u_v and d_v valence quark distributions:

$$\begin{aligned} {\sigma_p}^{\pi^+} - {\sigma_p}^{\pi^-} &\propto (D^+ - D^-)(4u_v - d_v) \\ {\sigma_d}^{\pi^+} - {\sigma_d}^{\pi^-} &\approx ({\sigma_p}^{\pi^+} - {\sigma_p}^{\pi^-}) + ({\sigma_n}^{\pi^+} - {\sigma_n}^{\pi^-}) \\ &\propto (D^+ - D^-)(3u_v + 3d_v), \end{aligned} \tag{12}$$

where $u_v = u - \bar{u}$, and $d_v = d - \bar{d}$. Of course, only the full parton distribution u (and d) is physical, but at intermediate to large x, $x > 0.3$, sea quark contributions are small and it is common to consider valence quark distributions only in this region.

The d_v/u_v ratio can be directly extracted from a specific combination of the measured proton and deuteron $\pi^\pm$ cross sections as follows:

$$R_{pd}^-(x) = \frac{\sigma_p^{\pi^+}(x,z) - \sigma_p^{\pi^-}(x,z)}{\sigma_d^{\pi^+}(x,z) - \sigma_d^{\pi^-}(x,z)} = \frac{4u_v(x) - d_v(x)}{3[u_v(x) + d_v(x)]}, \tag{13}$$

from which one finds

$$d_v/u_v = (4 - 3R_{pd}^-)/(3R_{pd}^- + 1). \tag{14}$$

Studying the x and z (and P_t) dependencies of R_{pd}^- and d_v/u_v thus provides an excellent test of the validity of the high-energy factorized view of the SIDIS process, and the various assumptions made.

The ratio of d_v/u_v from E00-108 is shown in Fig. 4, both as a function of x at z=0.55 (top panel), and as a function of z at x=0.32 (bottom panel). The ratios extracted from our SIDIS data are also compared to WA-21/25 data from neutrino and anti-neutrino deep inelastic scattering off proton targets (solid squares) [48], and to ratios extracted from forward hadron production data from the European Muon Collaboration (open squares) [3]. The shaded bands on both panels represent the values (including their present uncertainties) as calculated from Eq. 13 using CTEQ parton distribution functions [17].

The experimentally extracted ratios appear somewhat low as compared to the quark-parton model expectations using the CTEQ parton distributions, but possibly within uncertainties. For the results of the presented experiment, one should not only take into account experimental systematic uncertainties, but also possible biases due to various assumptions in low-energy factorization and symmetry in fragmentation functions, etc. Nonetheless, the E00-108 data (at $P_t \approx 0$) are in good agreement with previous extractions of WA21/25 and EMC, with vastly different techniques.

The undershoot as compared to CTEQ parton distribution function expectations can be further investigated by looking the dependence on z of the measured ratios at a fixed value of x (= 0.32). If isospin symmetry between favored (D^+) and unfavored (D^-) fragmentation functions of light quarks (u and d) and anti-quarks ($\bar{u}$ and $\bar{d}$) breaks down ($D_u^{\pi^+} \neq D_{\bar{u}}^{\pi^-} \neq D_d^{\pi^-} \neq D_{\bar{d}}^{\pi^+}$ and $D_u^{\pi^-} \neq D_{\bar{u}}^{\pi^+} \neq D_d^{\pi^+} \neq D_{\bar{d}}^{\pi^-}$), the ratios of Eq. 13 may contain additional z-dependent factors, related to asymmetries between the fragmentation functions. Thus, a dependence of the extracted "d_v/u_v ratio" on z will be a good indication for a breakdown of the symmetry assumptions, or of the factorized formalism. Indeed, one can witness in the bottom panel of Fig. 4 a sharp increase of the extracted d_v/u_v ratio at $z > 0.7$. This is likely not surprising as $z > 0.7$ corresponds in E00-108

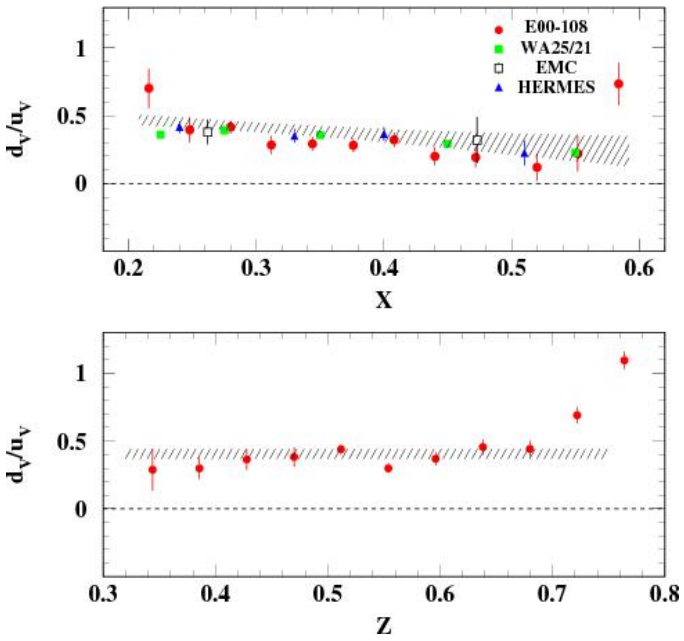

FIG. 4: (Color online) Top panel: The ratio of valence quarks d_v/u_v as a function of x at z=0.55. Solid circles are our data from E00-108 experiment (at $P_{h\perp} \approx 0$) after events from ρ decay are subtracted. Solid and open squares represent data from WA-21/25 [48] and EMC [3]. Solid triangle symbols are HERMES data [5] integrated over the $0.2 < z < 0.7$ range. Bottom panel: The ratio of valence quarks d_v/u_v as a function of z at x=0.32. Solid circles are our data from E00-108 after events from diffractive ρ decay are subtracted. The shaded bands on both panels reflect the values of and uncertainties in this ratio using CTEQ parton distribution functions, based on Eq. 13 [17].

kinematics to missing mass $M_x^2 < 2.5$ GeV^2), where *e.g.* the Δ- and higher-resonance contributions become dominant.

Below $z \approx 0.7$, the extracted d_v/u_v ratio is found to be reasonably independent of z, within the uncertainties of the data. On average, the data is somewhat low as compared to the quark-parton model expectations based upon CTEQ parton distribution functions, similar as was found in the x-dependence of this ratio.

Even though the extracted d_v/u_v ratios from the E00-108 experiment tend to undershoot the expectations based upon CTEQ6 parton distributions, the agreement with the existing WA21/25 and EMC data is good, and possibly points to the applicability of the assumed factorization and access to the quark-parton model in relatively low-energy SIDIS data. This is consistent with the findings in Ref. [16].

Nonetheless, one can also play devil's advocate and wonder why the SIDIS data tend to undershoot. The extracted d_v/u_v ratio tends to be very sensitive to the applicability (or not) of the assumed (x, z) factorization, hence warranting a thorough systematic study of the basic SIDIS pion electroproduction cross sections, *including* the π°, as a quantification of such factorization at JLab energies.

IV. EXPERIMENT

We propose to measure basic cross sections of the semi-inclusive π° electroproduction process off a proton target, at small transverse momentum (scale $P_{h\perp} \approx \Lambda$). These neutral-pion measurements will provide crucial input towards our validation of the basic SIDIS framework and data analysis at JLab energies, explicitly in terms of validation of anticipated (x, z) factorization.

In this experiment we plan to make coincidence measurements between scattered electrons in the existing HMS and photons from π° decay in a Neutral Particle Spectrometer (NPS) using a $PbWO_4$ calorimeter. The $PbWO_4$ calorimeter will detect photons corresponding to π° electroproduction close to the direction of $\vec{q}$ (parallel

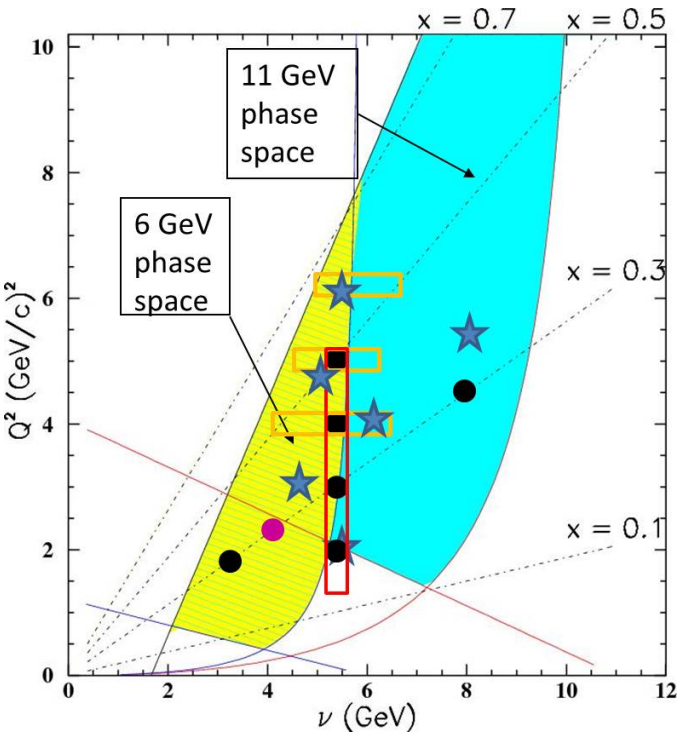

FIG. 5: *Q^2 versus x phase space available for semi-inclusive (or exclusive) coincidence experiments in Hall C at 11 GeV using the HMS and either the SHMS or the envisioned NPS. The stars indicate kinematics of proposed semi-inclusive π° production experiment.Other symbols indicate kinematics of the E00-108 (magenta circle), E12-09-017 (black circles), E12-06-104 (red box), E12-09-002 (yellow boxes) experiments.*

kinematics). These events correspond to θ_{π° near zero degrees, although, as will be shown later, we will have full (sufficient) coverage over ϕ_{π° up to transverse momentum of $P_{h\perp}$=0.3 (0.4) GeV and thus potentially eliminate any dependence on the interference terms.

We intend to perform all measurements on a hydrogen target, apart from the necessary Al "dummy" measurements for target wall subtraction. The experiment will use an 11-GeV beam energy to map a region in Bjorken x between 0.2 and 0.5, in z between 0.4 and 0.8, and in θ_{pq} to cover a range in $P_{h\perp}$ up to 0.4 GeV. To better constrain the possible (x, z) entanglement, we plan to measure over a range in Q^2 for *fixed* value of x = 0.36, while still varying z. All kinematics are compatible with a companion DVCS/DVNP proposal, and part of the run group, a novelty within Hall C.

A. Choice of Kinematics

We plan to map the semi-inclusive neutral-pion electroproduction process off the proton target in a (x, Q^2) phase space compatible with the measurements approved for semi-inclusive charged-pion electroproduction as approved in E12-09-017. The HMS spectrometer setting (with the choice of 11 GeV beam energy) will determine the (x, Q^2) of the specific kinematics. The large solid angle (25 msr) and full momentum acceptance of the NPS will then allow to map the z, and $P_{h\perp}$ dependence, typically for a range of z between 0.4 and 0.8 and a range of $P_{h\perp}$ up to 0.3-0.4 GeV.

We will measure the semi-inclusive neutral-pion electroproduction yields over the range in z and θ_{pq} for five kinematics, $A - F$ (see Table III and IV).

Figure 5 shows the accessible Q^2-x_B phase space for 12 GeV experiments in Hall C for exclusive and semi-inclusive kinematics, with the specific kinematics added where charged-pion SIDIS data are anticipated

TABLE III: Kinematic settings, with HMS providing the electron spectrometer and NPS the neutral-pion spectrometer.

Kinematics	E (GeV)	E' (GeV)	θ_e (deg)	W^2 (GeV^2)	θ_γ (deg)	q_γ (GeV)	x	Q^2 (GeV^2)	z
A	11.0	5.67	10.27	8.88	10.57	5.513	0.20	2.0	0.4−0.8
B	11.0	6.56	11.70	6.21	16.20	4.767	0.36	3.0	0.5−0.8
C	11.0	5.08	15.38	7.99	12.44	6.250	0.36	4.0	0.4−0.8
D	11.0	2.86	24.15	10.66	7.93	8.472	0.36	5.5	0.3−0.8
E	11.0	5.88	15.65	5.68	16.57	5.565	0.50	4.8	0.4−0.8
F	11.0	5.67	17.84	4.88	17.23	5.865	0.60	6.0	0.4−0.8

and neutral-pion SIDIS data from this proposal. The minimum laboratory angle of HMS is 10.5°. For the first kinematics, at $(x,\ Q^2) = (0.20,\ 2.00\ \text{GeV}^2)$, we will park the HMS at 10.5° and benefit from the ≈3° angular acceptance of HMS to cover the nominal 10.27° scattering angle. The NPS minimum angle is 7.93°, well beyond the envisioned smallest-angle reach of NPS of 5.5°, also alleviating backgrounds. The range in z while $M_x^2 > 2.5$ GeV^2 is up to about $z = 0.7$-0.8. Given that the nucleon resonance contributions for $ep \to e'\pi^\circ\Delta^+$ are reduced as compared to $ep \to e'\pi^-\Delta^{++}$, the $M_x^2 > 2.5$ GeV^2 constraint may be relaxed.

In Fig. 6 we illustrate the $(P_{h\perp}, \phi)$ coverage for the various kinematics A-F. Sufficient coverage in ϕ is obtained up to $P_{h\perp}$ of 0.3 (0.4) GeV, to potentially remove any sensitivity to interference structure functions in SIDIS kinematics by integration, or alternatively determine $\cos(\phi)$ or $\cos(2\phi)$ moments.

In the appendix we have included the general kinematics overview Table VI of the companion proposed DVCS/DVNP experiment. We have added one row in the bottom to clarify what the proposed SIDIS kinematics A-F correspond to. SIDIS data would be accumulated simultaneously with the proposed DVCS/DVNP experiment. We note that the exact distance of the calorimeter is still under discussion, and is linked to the final sweeping magnet design. For SIDIS, we have assumed a generic distance of 4 meters, which works well with the present magnet design under discussion. The shorter distance of 3 meters would also benefit the SIDIS experiments and give somewhat larger $P_{h\perp}$ coverage, but will require a revisit of the magnet design as presently under consideration. For the NPS angles required for the SIDIS kinematics, this seems possible.

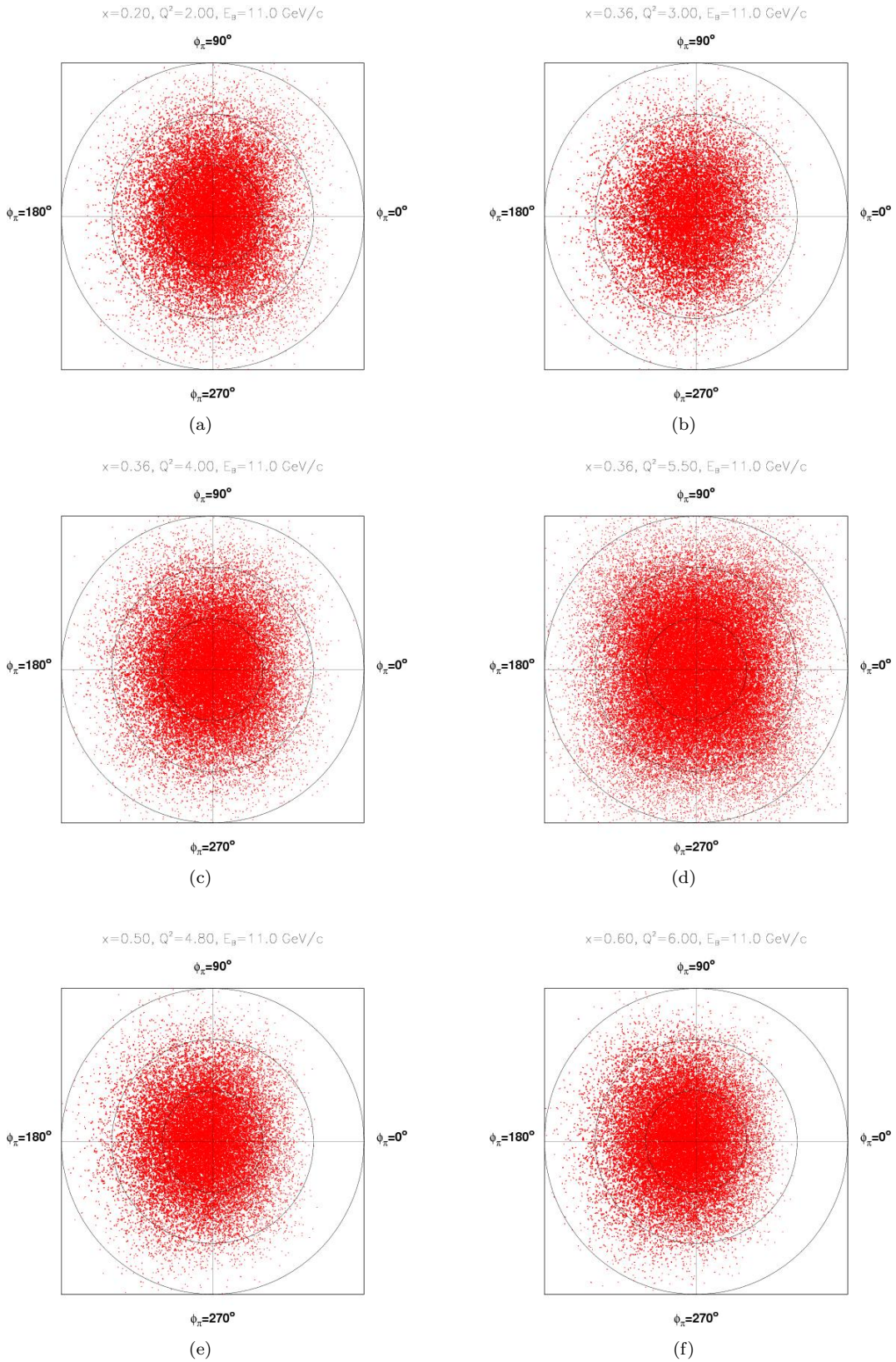

(a) (b) (c) (d) (e) (f)

FIG. 6: Coverage of proposed measurements in transverse momentum $P_{h\perp}$ and azimuthal angle ϕ. The plots are for the kinematics (a):($x,\ Q^2$) = (0.20, 2.00 GeV^2); (b):($x,\ Q^2$) = (0.36, 3.00 GeV^2); (c):($x,\ Q^2$) = (0.36, 4.00 GeV^2); (d):($x,\ Q^2$) = (0.36, 5.50 GeV^2); (e):($x,\ Q^2$) = (0.50, 4.80 GeV^2) and (f):($x,\ Q^2$) = (0.60, 6.00 GeV^2) . The circles indicate $P_{h\perp}$ = 0.2, 0.4, and 0.6 GeV, respectively.

TABLE IV: Kinematic settings and expected coincidence counts within $\triangle z$=0.1 bins for the Semi-Inclusive $(e, e'\pi^\circ)X$ production measurements. The NPS is positioned along the virtual photon direction as caluclated from central kinematics. The beam energy is 11 GeV. Beam current is assumed to be 1 μA, and the target is assumed to be 10 cm LH2 for the rate estimates. Rates are given in kilo-counts per hour, with the "detected" column taking into account the geometric π° detection effficiency.

Kinematics	E (GeV)	E' (GeV)	θ_e (deg)	x	Q^2 (GeV^2)	W (GeV)	θ_γ (deg)	q_γ (GeV/c)	$\pi^\circ - eff$ (%)	z	k-counts/h expected	k-counts/h detected
A	11.0	5.67	10.27	0.20	2.00	2.98	10.57	5.513	1.0	0.30	26.11	0.261
									9.3	0.40	29.89	2.780
									19.9	0.50	30.37	6.109
									29.5	0.60	27.23	8.033
									38.0	0.70	21.15	8.037
									45.4	0.80	12.37	5.616
B	11.0	6.56	11.70	0.36	3.00	2.49	16.21	4.767	0.0	0.30	10.87	0.054
									3.0	0.40	12.66	0.380
									11.1	0.50	13.06	1.450
									19.9	0.60	11.83	2.354
									28.0	0.70	9.30	2.604
									35.3	0.80	5.99	2.114
C	11.0	5.08	15.38	0.36	4.00	2.83	12.44	6.250	3.0	0.30	3.92	0.118
									14.1	0.40	4.45	0.627
									25.5	0.50	4.46	1.137
									35.3	0.60	3.93	1.387
									43.8	0.70	3.00	1.314
									51.1	0.80	1.86	0.950
D	11.0	2.86	24.14	0.36	5.50	3.26	7.93	8.472	15.6	0.30	0.68	0.106
									30.6	0.40	0.73	0.223
									42.7	0.50	0.70	0.299
									52.8	0.60	0.58	0.306
									61.0	0.70	0.42	0.256
									68.2	0.80	0.25	0.171
E	11.0	5.88	15.65	0.50	4.80	2.38	16.57	5.565	0.5	0.30	2.10	0.011
									7.7	0.40	2.45	0.189
									17.9	0.50	2.47	0.442
									27.3	0.60	2.21	0.603
									35.7	0.70	1.71	0.610
									43.0	0.80	1.08	0.464
F	11.0	5.67	17.84	0.60	6.00	2.21	17.23	5.865	1.0	0.30	0.75	0.008
									9.3	0.40	0.86	0.080
									20.0	0.50	0.87	0.174
									29.6	0.60	0.77	0.228
									38.0	0.70	0.59	0.224
									45.4	0.80	0.37	0.168

B. Physics Singles Rates and Physics Backgrounds

Singles rates from (e, π°) and (e, e') can result in accidental coincidences which are a source of background for the measurement. However, as compared to the magnetic spectrometer setup planned for various $(e, e'\pi^\pm)$ experiments in Hall C (E12-06-104, E12-07-105, E12-09-011, E12-09-017) the beam current assumption ($\sim$ few μA) is modest as compared to the more typical >50 μA of the mentioned experiments, with similar length cryogenic targets. This implies a negligible accidental coincidence rate of about 2-10%, which can be easily

TABLE V: *Estimated systematic uncertainties for the π° cross section measurements based on previous Hall C experiments. We have remained separation between point-to-point uncertainties, relevant for separated structure functions, and scale uncertainties. It is important to realize that the HMS is a very well understood magnetic spectrometer which will be used in modest requirements (beyond the momentum), defining the (x, Q^2) kinematics well. The pt-to-pt (scale uncertainties) for radiative corrections and Monte Carlo model are 1% (2%) and 0.2% (1%), and should be added in quadrature in the total.*

Source	pt-to-pt (%)	scale (%)
Acceptance	0.4	1.0
Electron PID	<0.1	<0.1
π° efficiency [a]	1.0	1.0
Electron tracking efficiency	0.1	0.5
Charge	0.5	2.0
Target thickness	0.2	0.5
Kinematics	0.3	<0.1
Total (including rad, mod)	1.6	3.4
Total	1.2	2.5

[a]includes combinatoric background

subtracted.

The singles rate in the HMS is in fact expected to be less than 2 kHz (or 4 kHz for the series of kinematics utilizing LD2 targets). Hence, projected rates for the HMS are low and are well within the operating parameters of previous HMS experiments. In this experiment, the π/e ratio in the HMS is never larger than 130:1, even without reducing this ratio at the hardware trigger level. The electron will be identified using the lead-glass calorimeter in combination with the gas Cherenkov.

The singles rates in the neutral-pion detector are dominated by background. This was simulated and is discussed in detail in a dedicated writeup for the NPS.

We have chosen a liquid hydrogen target with a length of 10 cm. This means that the target end windows will be in the acceptance of the spectrometers (HMS and NPS) in all configurations, and the background subtractions are necessary. Background events from the target end windows will be measured in "empty" target runs. The Hall C empty target consists of two thin Aluminum pieces separated by a length equivalent to the cryogenic target length. However, the empty target is thicker by a factor of 6-7 relative to the target cell walls, a thickness chosen to make the radiation lengths of LH2 (plus windows) and these "empty" targets about equivalent. The thicker target allows for a more rapid accumulation of counts for these background subtraction measurements. These short measurements are implicitly included in the beam time request.

C. Systematic Uncertainties

The estimated systematic uncertainties for the $(e, e'\pi^\circ)$ reaction are listed in Table V. These are largely based on the previous experience with the HMS+SOS spectrometer pair in Hall C, and we benefit from the well-understood HMS that will determine the (x, Q^2) kinematics allowing for the L/T separation program. In fact, in comparison to the recent coincidence measurements in which the electron was detected in the SOS, we expect some improvements in the contributions to the systematic uncertainty. For example, the HMS acceptance is much flatter than the SOS acceptance. The neutral-pion acceptance is fully given by geometry and not prone to magnetic field knowledge at all. Tracking efficiency knowledge in the HMS is expected to be excellent at the low rates anticipated in this experiment. In the case of π° detection, the calorimeter performance is expected to be comparable to the one in the PRIMEX-II experiment, with detailed understanding.

Some uncertainties will be larger than, for instance, those projected for the charged-pion L/T separations

in electroproduction and the pion form factor measurements at 12 GeV. First of all, the beam current can be as low as 1 μA. We conservatively assume a 2% scale uncertainty (this may be reduced to 1% with a lead-tungsten calorimeter under consideration), and a 0.5% relative measurement of the collected beam charge. Of course, we note that in the semi-inclusive data analysis only the ratio of $(e, e'\pi^\circ)$ and (e, e') yields is relevant, with absolute beam current knowledge dropping out.

Secondly, we plan to use the HMS spectrometer up to a momentum of 6.6 GeV/c, some 10% below its maximum design momentum of 7.3 GeV/c. Data taking at a 6-GeV Jefferson Lab has shown an excellent and stable performance and detailed understanding of this for HMS momentum up to $\sim$ 5.5 GeV/c. Some saturation effects are anticipated in the magnetic performance equivalent to a central momentum of 6.6 GeV/c. The anticipated behavior in the HMS quadrupole magnets has been mapped through rotating-coil measurements in the early 1990s, but exact implications for the understanding of the HMS optics and acceptance require data. Luckily, the implications are expected to be minor as compared to the magnetic field saturation effects one had to face with the SOS for the earlier 6-GeV precision L/T separation program in Hall C. Even more, we only plan to use the HMS at angles below 25° with a modest 10 cm long target, which essentially acts as a point target for HMS optics. Nonetheless, we have retained a 1% scale uncertainty in the understanding of the acceptance of the HMS.

Thirdly, some variation of the gain of the PMTs, and degradation of the $PbWO_4$ crystals during the experiment is anticipated. To minimize variation in the PMT gains at high rates (as observed in PRIMEX) we will use active bases with built-up pre-amplifiers which powered from a high-voltage division chain [49]. This active base will allow for operating the PMTs at lower voltages and lower anode currents, with gain stability better than $\sim$1% for the rates up to $\sim$1.5 MHz. Nevertheless we have included a projected 1% nonlinearity in gain leading to the projected 1% of "PID" (π° PID and efficiency) in Table V. This is far more conservative than the achieved knowledge from the PRIMEX-II experience.

Lastly, well-established models for separated pion electroproduction cross sections above the resonance region do not exist, and there will thus be equivalent uncertainty in the radiative correction estimates. Even if reduced due to the less prominent role of the nucleon resonances in the π° channel (as compared to π^+), this may be the largest single systematic uncertainty for the proposed experiment. This can be reduced through further data accumulation for this process with 12-GeV experiments.

V. SUMMARY AND BEAM TIME REQUEST

We request a total of 25 days of beam time to measure basic cross sections for semi-inclusive electroproduction of neutral pions from a proton target, to a level of 3% precision. The cross section measurements will cover a range compatible with the approved charged-pion basic cross section program, $0.2 < x < 0.5$, $2 < Q^2 < 5$ GeV^2, $0.4 < z < 0.8$, and $P_{h\perp} < 0.4$ GeV, and will provide a firm basis to validate our understanding of the (x, z) factorization in the SIDIS framework at a 12-GeV JLab. This will shed light on various potential analysis pitfalls, and provide the foundation for a solid interpretation of any semi-inclusive deep inelastic scattering data within a partonic description.

We plan to perform such (e,e$'\pi^\circ$) coincidence measurements utilizing the well-understood HMS with a new Neutral-Pion Spectrometer facility. We request a polarized electron beam to add the possibility to determine single-spin asymmetries from these measurements.

This proposal is part of a rungroup with a companion DVCS/DVNP proposal, and thus provides a unicum within Hall C. The 25 days of beam time request are fully compatible with the DVCS/DVNP companion proposal, and assume a beam current ranging from 1 to 20 μA, and a 10 cm LH2 target, with a base beam energy of 11.0 GeV. The days of beam time request are driven by the companion DVCS/DVNP proposal and assume for kinematics A-F one day, one day, three days, five days, five days, and ten days, respectively. For this SIDIS proposal this will render 10K events for each z bin, even at a conservative beam current of 1 μA.

[1] R. Asaturyan *et* al., Phys. Rev. C **85** (2012) 015202.

[2] Neutral Particle Spectrometer Facility in Hall C. Proposal to Jefferson Lab PAC40; https://hallcweb.jlab.org/experiments/PAC40/nps.pdf, Contact person T. Horn.

[3] J. Ashman *et al.*, Phys. Lett. **B 206**, 364 (1988), Nucl. Phys. **B 328**, 1 (1989).

[4] P. L. Anthony *et al.*, Phys. Lett. **B 458**, 529 (1999); **B 463**, 339 (1999); **B 493**, 19 (2000).

[5] A. Airapetian *et al.*, Phys. Lett. **B 404**, 383 (1997); **B 444**, 531 (1998); **B 442**, 484 (1998).

[6] J. Adams *et al.*, Phys. Rev. Lett. **92**, 171801 (2004); S. S. Adler *et al.*, Phys. Rev. Lett. **91**, 241803 (2003).

[7] A. Accardi, T. Hobbs, and W. Melnitchouk, JHEP 0911 (2009) 084.

[8] F.E. Close and W. Melnitchouk, Phys. Rev. C **79** (2009) 055202

[9] J. T. Dakin, G. J. Feldman, F. Martin, M. L. Perl, and W. T. Toner, Phys. Rev. Lett. **31**, 786 (1973).

[10] M. Stratmann and W. Vogelsang, Nucl. Phys. **B496**, 41 (1997); D. de Florian and R. Sassot, Phys. Rev. D **56**, 426 (1997).

[11] A. S. Raskin and T. W. Donnelly, Ann. Phys. (N.Y.) **191**, 78 (1989).

[12] J. Binnewies, B. A. Kniehl, and G. Kramer, Phys. Rev. D **52**, 4947 (1995).

[13] E. L. Berger, Nucl. Phys. **B85**, 61 (1975).

[14] E. L. Berger, Proc. of the Workshop on Electronuclear Physics with Internal Targets, Stanford, CA, January 5-7, 1987.

[15] P. J. Mulders, in: R. G. Milner (Ed.), EPIC 2000: Proceeding of the 2nd Workshop on Physics with an Electron Polarized Light Ion Collider, Cambridge, MA, 2000; arXiv:hep-ph/0010199v1, 2000.

[16] T. Navasardyan *et al.*, Phys. Rev. Lett. **98** (2007) 022001.

[17] H. L. Lai, J. Huston, S. Kuhlmann, J. Morfin, F. Olness, J. F. Owens, J. Pumpin and W. K. Tung, Eur. Phys. J. C **12**, 375 (2000).

[18] X. Ji, J.-P. Ma, F. Yuan, Phys. Lett. **B597**, 299 (2004).

[19] P.J. Mulders and R.J. Tangerman, Nucl. Phys. **B461**, 197 (1996).

[20] A. Bachetta, M. Diehl, K. Goeke, A. Metz, P.J. Mulders, and M. Schlegel, JHEP **0702**, 093 (2007).

[21] M. Anselmino *et al.*, Eur. Phys. J. **A47**, 35 (2011).

[22] R.N. Cahn, Phys. Lett. **B78**, 269 (1978); Phys. Rev. **D40**, 3107 (1989)

[23] M. Anselmino, M. Boglione, U. D'Alesio, A. Kotzinian, F. Murgia and A. Prokudin, AIP Conf. Proc. **792**, 981 (2005) [arXiv:hep-ph/0507157]; M. Anselmino, M. Boglione, A. Prokudin and C. Turk, Eur. Phys. J. A **31**, 373 (2007) [arXiv:hep-ph/0606286]; M. Anselmino *et al.*, Phys. Rev. **D71** (2005) 074006; M. Anselmino, M. Boglione, A. Prokudin, and C. Turk, Eur. Phys. J. **A31** (2007) 373.

[24] A. Airapetian *et al.*, Phys. Rev. D **87** (2013) 012010.

[25] G. Sbrizzai *et al.*, J. Phys. Conf. Ser. **295** (2011), 012043; DIS2013 presentation (2013), see https://indico.cern.ch/contributionDisplay.py?sessionId=7&contribId=224&confId=184503.

[26] H. Mkrtchyan *et al.*, Phys. Lett. **B665** (2008) 20.

[27] M. Wakamatsu, Phys. Rev. **D79** (2009) 094028.

[28] P. Schweitzer, T. Teckentrup, and A. Metz, Phys. Rev. D **81**, 094019 (2010).

[29] M. Osipenko *et al.*, Phys. Rev. D **80**, 032004 (2009).

[30] T. Sjostrand, S. Mrenna, and P. Z. Skands, JHEP 05 (2006) 026; T. Sjostrand, L. Lonnbland, S. Mrenna, and P. Z. Skands, arXiv:hep-ph/0308153v1.

[31] P. Liebing, Ph.D. dissertation, University of Hamburg, 2004.

[32] C. Hadjidakis, Ph.D. dissertation, Institut de Physique Nucleaire Orsay, 2002.

[33] H. Avagyan (private communication).

[34] L. W. Mo and Y. S. Tsai, Rev. Mod. Phys. **41**, 205 (1969).

[35] R. Ent, B. Filippone, N. C. R. Makins, R. G. Milner, T. G. O'Neill and D. A. Wasson, Phys. Rev. C **64**, 054610 (2001).

[36] D. M. Koltenuk, Ph.D. thesis, University of Pennsylvania, 1999.

[37] D. Gaskell, Ph.D thesis, Oregon State University, 2001.

[38] I. Akushevich, A. Ilyichev, N. Shumeiko, A. Soroko, A. Tolkachev, Comp. Phys. Comm. **104**, 201 (1997).

[39] T. V. Kuchto and N. M. Shumeiko, Nucl. Phys. **B219**, 412 (1983).

[40] I. Akushevich and N. M. Shumeiko, J. Phys. G: Nucl. Part. Phys. **20**, 513 (1994).

[41] P. Brauel, T. Canzler *et al.*, Z. Physik C **3**, 101 (1979).

[42] H. P. Blok *et al.*, Phys. Rev. C **78**, 045202 (2008).
[43] V. Tadevosyan *et al.*, Phys. Rev. C **75**, 055205 (2007).
[44] T. Horn *et al.*, Phys. Rev. Lett. **97**, 192001 (2006).
[45] D. Drechsel, S. S. Kamalov, and L. Tiator, Nucl. Phys. **A645**, 145 (1999).
[46] I. Akushevich, N. Shumeiko, and A. Soroko, Euro. Phys. J. C **10**, 681 (1999).
[47] E. Garutti, Ph.D. Dissertatio, Amsterdam University (2003).
[48] G. Jones *et al.*, Z. Phys. C **62**, 601 (1994).
[49] V. Popov, H. Mkrtchyan, New potomultiplier active base for Hall C Jefferson Lab Lead Tungstate Calorimeter, NSSS2012-1098.

VI. APPENDIX

In this appendix we have included the general kinematics overview Table VI of the companion proposed DVCS/DVNP experiment. We have added one row in the bottom to clarify what the proposed SIDIS kinematics A-F correspond to. SIDIS data would be accumulated simultaneously with the proposed DVCS/DVNP experiment.

TABLE VI: DVCS Kinematics for Hall C. The incident and scattered beam energies are k and k', respectively. The calorimeter is centered at the angle $\theta_{\rm Calo}$, which is set equal to the nominal virtual photon direction. The front face of the calorimeter is at a distance $D_{\rm Calo}$ from the center of the target, and is adjusted to optimize multiple parameters: First to maximize acceptance, second to ensure sufficient separation of the two clusters from symmetric $\pi^0 \to \gamma\gamma$ decays, and third to ensure that the edge of the calorimeter is never at an angle less than 3.2° from the beam line. The last row indicates the kinematics that are used simultaneously for this proposal, corresponding to the total request of 25 days. Kinematics that would be of general interest to push the Q^2 range of SIDIS experiments, but beyond the scope of the presently considered JLab SIDIS program, are marked with a G-I.

	Energy Dependence at fixed (Q^2, $x_{\rm Bj}$)												Low-$x_{\rm Bj}$				High-Q^2		
$x_{\rm Bj}$	0.36			0.50				0.60					0.2				0.36	0.50	0.60
Q^2 (GeV)^2	3.0			4.0		3.4		4.8	5.1			6.0	2.0			3.0	5.5	8.1	10
k (GeV)	6.6	8.8	11	8.8	11	8.8	11	11	6.6	8.8	11	11	6.6	8.8	11	11	11		
k' (GeV)	2.2	4.4	6.6	2.9	5.1	5.2	7.4	5.9	2.1	4.3	6.5	5.7	1.3	3.5	5.7	3.0	2.9	2.4	2.1
$\theta_{\rm Calo}$ (deg)	11.7	14.7	16.2	10.3	12.4	20.2	21.7	16.6	13.8	17.8	19.8	17.2	6.3	9.2	10.6	6.3	7.9	8.0	8.0
$D_{\rm Calo}$ (m)	3	3	3	4	3	3	3	3	3	3	3	3	6	4	4	6	4	4	4
Days	1	2	1	1	3	3	2	5	5	1	5	10	1	1	1	1	5	5	12
SIDIS			B		C			E				F			A	G	D	H	I

We have chosen kinematics A-F of this proposal to be overlapping the approved unpolarized cross section and azimuthal asymmetry measurement phase space of SIDIS experiments in Hall C. Nonetheless, some additional kinematics could provide important information for possible later SIDIS studies where one pushes to the corners of allowable phase space (in Q^2) at a 12-GeV JLab. These kinematics are indicated as G, H, and I, with more information on coincidence rates given in Table VII. We would foresee to take parasitic SIDIS data in these kinematics might the proposed DVCS/DVNP experiment be (hopefully) approved, albeit at reduced statistics per z bin.

TABLE VII: Additional possible Kinematic settings (overlapping with other experiments) and expected coincidence counts within $\triangle z$=0.1 bins for the Semi-Inclusive $(e, e'\pi^\circ)X$ production measurements. Pions are along the virtual photon direction. The NPS is positioned along the virtual photon direction as caluclated from central kinematics. The beam energy is 11 GeV. Beam current is assumed to be 1 μA, and the target is assumed to be 10 cm LH2 for the rate estimates. Rates are given in kilo-counts per hour, with the detected column taking into account the geometric π° detection effficiency.

Kinematics	E (GeV)	E' (GeV)	θ_e (deg)	x	Q^2 (GeV^2)	W (GeV)	θ_γ (deg)	q_γ (GeV/c)	$\pi^\circ - eff$ (%)	z	k-counts/h expected	k-counts/h detected
G	11.0	3.01	17.32	0.20	3.00	3.59	6.28	8.179	14.6	0.30	3.59	0.524
									29.6	0.40	3.93	1.163
									41.8	0.50	3.78	1.580
									51.8	0.60	3.18	1.647
									60.2	0.70	2.31	1.391
									67.2	0.80	1.37	0.921
H	11.0	2.37	32.39	0.50	8.10	3.00	8.02	9.090	18.5	0.30	0.12	0.022
									33.6	0.40	0.13	0.044
									45.9	0.50	0.12	0.055
									56.0	0.60	0.10	0.056
									64.3	0.70	0.07	0.045
									71.3	0.80	0.04	0.029
I	11.0	2.12	38.24	0.60	10.00	2.75	7.99	9.428	19.9	0.30	0.03	0.006
									35.3	0.40	0.04	0.014
									47.6	0.50	0.03	0.014
									57.5	0.60	0.03	0.017
									65.7	0.70	0.02	0.013
									72.6	0.80	0.01	0.007